

Intra- and inter-network interactions in magnetic oxides

O. Peña^{a,*}, C. Moure^b, P. Barahona^{a,c}, M. Baibich^d, G. Martinez^d

^a*Sciences Chimiques de Rennes, UMR 6226, CNRS—Université de Rennes 1, 35042 Rennes, France*

^b*Departamento de Electrocerámicas, Instituto de Cerámica y Vidrio, CSIC, Madrid, Spain*

^c*Departamento de Química, Facultad de Ciencias, Universidad de Chile, Santiago, Chile*

^d*Institute of Physics, UFRGS, Porto Alegre, Brazil*

Abstract

Partial substitutions of Mn by a transition metal Me in the rare-earth manganites $\text{REMe}_x\text{Mn}_{1-x}\text{O}_3$ results in the simultaneous presence of Mn^{3+} and Mn^{4+} , triggering double exchange ferromagnetic mechanisms. The RE sublattice has its own properties and can interact with the local field imposed by the ferromagnetic network. Its orientation differs depending on the RE nature, adopting most usually a parallel (additive) direction with respect to the (applied + local) field but, in other cases, it may align in an opposite direction, resulting in an uncompensated antiferromagnetic lattice and a reversal of the magnetic moment (spin inversion) during thermal cycling. A particular case concerns the half-substituted compound $\text{ErCo}_{0.50}\text{Mn}_{0.50}\text{O}_3$ for which the magnetization loop presents two well-identified anomalies, at high field (metamagnetic or spin-flop transition) and at low field (intersection of the magnetization branches).

Keywords: Magnetic oxides; Exchange interactions; Spin inversion

1. Introduction

Presence of two well-defined crystallographic and magnetic sublattices in the $(\text{RE},\text{A})\text{MnO}_3$ manganites (RE = rare earth, A = alkaline earth) leads to interesting features, due to the relative orientations of their respective magnetic moments. If the exchange interaction J between networks is negative and, in addition, the magnitude of the rare-earth moment is much higher than the one due to the ferromagnetic Mn lattice, a ferrimagnetic-like state occurs, which may lead to unusual situations. Thus, a net inversion of the magnetization has been reported in $(\text{Gd},\text{Ca})\text{MnO}_3$ and $(\text{Dy},\text{Ca})\text{MnO}_3$ [1–3].

Double-exchange interactions may also be enhanced by substitutions at the Mn site since a transformation $\text{Mn}^{3+} \rightarrow \text{Mn}^{4+}$ will take place. If the substituent is a divalent ion Me, the general formulation will be $\text{RE}^{3+}\text{Me}^{2+}_x\text{Mn}^{3+}_{(1-x)}\text{Mn}^{4+}_x\text{O}_3^{2-}$ and the solid solution will be limited to $x = 0.50$. If the substituent Me presents two

stable oxidation states (e.g., Co) then, the solid solution may extend beyond the threshold $x = 0.5$, reaching 0.6 or 0.7 cobalt atoms in $\text{YCo}_x\text{Mn}_{1-x}\text{O}_3$ [4].

In order to investigate the spin reversal phenomenon in perovskites with a partially substituted manganese network, we synthesized two series of compounds $\text{RE}(\text{Me}, \text{Mn})\text{O}_3$, where RE = Gd or Er. Preliminary results were presented for a limited number of $\text{Gd}(\text{Ni},\text{Mn})\text{O}_3$ and $\text{Gd}(\text{Cu},\text{Mn})\text{O}_3$ compositions [5]. In this work, data for $\text{GdCo}_x\text{Mn}_{1-x}\text{O}_3$ ($x \leq 1$) and $\text{ErCo}_x\text{Mn}_{1-x}\text{O}_3$ ($x \leq 0.7$) are presented, emphasizing the magnetic aspects and comparing results with the $\text{Gd}_{1-x}\text{Ca}_x\text{MnO}_3$ and $\text{Er}_{1-x}\text{Ca}_x\text{MnO}_3$ series, in which the substitution was done at the lanthanide site.

2. Experimental

Samples were prepared by solid-state reaction of reagent grade MnO , CoO , Gd_2O_3 and Er_2O_3 oxides with sub-micronic particle size. The mixtures were homogenized by attrition milling in isopropanol and calcined at 1150°C for 2 h. They were further re-milled, dried, granulated and

*Corresponding author. Tel.: +33 2 23 23 67 57; fax: +33 2 23 23 67 99.
E-mail address: peña@univ-rennes1.fr (O. Peña).

uniaxially pressed. Sintering was performed at temperatures ranging between 1325 and 1450 °C, the lowest corresponding to the highest Co amount. For contents higher than 50 at % Co, samples were sintered in O₂ atmosphere, with a cooling rate of 1 °C/min. Densities higher than 96% theoretical were attained for all samples. X-ray diffraction was performed using a D-5000 Siemens diffractometer with CuK_α radiation and Ni filter. All samples show a perovskite orthorhombic structure, space group Pbnm; lattice parameters are given elsewhere. Magnetic measurements were performed in a Quantum Design MPMS-XL5 SQUID susceptometer, between 2 and 300 K and under magnetic fields ranging from -50 to +50 kOe.

3. Results and discussion

3.1. Paramagnetic state

Fig. 1 shows some data obtained in typical samples of the series GdCo_xMn_{1-x}O₃ and ErCo_xMn_{1-x}O₃. The high-temperature region is characterized by a linear variation of χ^{-1} with temperature, while a larger decrease occurs at the approach of the magnetically ordered state (for this reason, data is shown as the ratio $(M/H)^{-1}$, since the magnetization at low temperatures is not linear anymore with the magnetic field). The paramagnetic state does not depend on the annealing conditions (insert, Fig. 1); however, important modifications of the magnetization loops are observed in the ordered state, as will be discussed in Section.3.3.

The paramagnetic data were then fitted by a Curie-Weiss law in the range $1.5T_c \leq T \leq 300$ K, where the ordering temperature T_c is defined as the lowest temperature of the reversible state ($T_c = T_{rev}$; see below) [2]. Table 1 summarizes the magnetic parameters for both series. Several tendencies can be remarked: first of all, the ordering temperatures T_c for the GdCo_xMn_{1-x}O₃ series

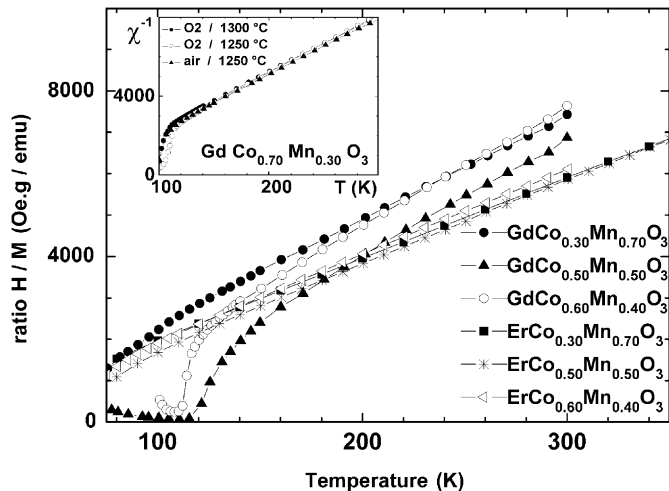


Fig. 1. Thermal dependence of the ratio $(M/H)^{-1}$. Insert shows data for GdCo_{0.70}Mn_{0.30}O₃ after different annealings.

Table 1

Magnetic data for the GdCo_xMn_{1-x}O₃ and ErCo_xMn_{1-x}O₃ series. Data fitted by a Curie-Weiss law in the range $1.5T_c \leq T \leq 300$ K

$x(\text{Co})$	T_c (K) ± 3	Θ (K)	μ_{eff} (μ_B) ± 0.15	$\mu_{\text{Mn+Co}}$ (μ_B)
GdCo _x Mn _{1-x} O ₃				
0.25	50	+1.7 \pm 0.3	9.26	4.77
0.30	85	+5.2 \pm 0.5	9.12	4.49
0.45	115	+35 \pm 2	8.57	3.23
0.50	120	+58 \pm 3	8.61	3.33
0.60	110	+36 \pm 1	8.52	3.09
0.70	100	+20 \pm 1	8.52	3.09
0.80	100	+9 \pm 1	8.37	2.65
0.90	50	+1.7 \pm 0.5	8.34	2.55
1.0	190	-10 \pm 5	8.70	3.56
ErCo _x Mn _{1-x} O ₃				
0.20	50	-11 \pm 0.5	10.47	4.22
0.30	55	-4.5 \pm 1	10.52	4.35
0.33	55	-2 \pm 0.5	10.48	4.25
0.40	62	+5 \pm 2	10.26	3.67
0.50	68	+13 \pm 1	10.14	3.32
0.60	68	+10 \pm 1	10.16	3.38
0.70	67	+1.3 \pm 0.5	10.19	3.47

are about twice as large as the ones for the ErCo_xMn_{1-x}O₃ series. Secondly, the maxima in the characteristic temperatures (either T_c or Θ values), are situated around the composition 50/50 = Mn/Co, for which charge ordering, can be expected as observed in the Y(Ni,Mn)O₃ perovskites [6]. The antiferromagnetic character of the matrix can be observed at both ends of the erbium and gadolinium series, where Θ goes toward negative values.

The lanthanide ($\mu_{\text{eff}}^{\text{Er}}$ and $\mu_{\text{eff}}^{\text{Gd}}$) contributions were subtracted in the usual way [2]. The resulting magnetic moment (Table 1), which corresponds to the added contribution of the transition metals, is in general, lower than the expected values for any combination of the Mn and Co moments (3.87 μ_B for Mn⁴⁺ and Co²⁺; 4.90 μ_B for Mn³⁺ and Co³⁺), unless an antiferromagnetic interaction is assumed between them. This fact suggests that the cobalt spins are oriented antiparallel to the manganese moments, enhancing the antiferromagnetic component (see below).

3.2. Spin reversal

The ordered regime was investigated by performing magnetization cycles as a function of temperature (ZFC/FC) and applied field (magnetization loops). Fig. 2 (upper and middle panels) shows typical ZFC/FC data obtained under an external field of 250 Oe. When first warming the sample (ZFC process), a small decrease of the magnetization is observed, due mainly to the magnetic contribution of the lanthanide moments. This decrease is more pronounced in the case of erbium since its free ion moment is higher than the one of gadolinium (9.58 μ_B and 7.94 μ_B , for Er³⁺ and Gd³⁺, respectively). Upon further warming, the magnetization $M(T)$ goes through well-defined maxima at $T = T_{\text{max}}$. This process is attributed to the canted-type magnetic structure of the transition-metal network, where

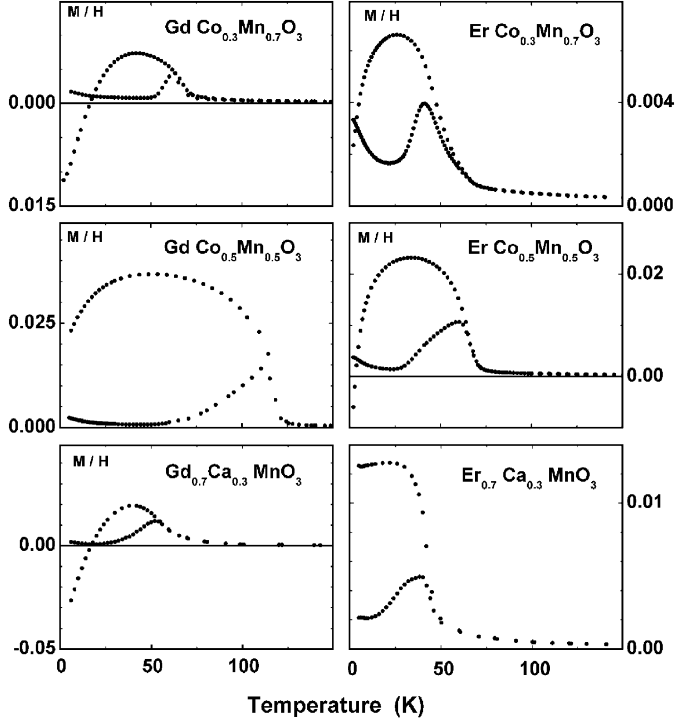


Fig. 2. ZFC/FC magnetization normalized to the magnetic field (units of emu/g Oe) performed at $H_{app} = 250$ Oe.

antiferromagnetic inter-plane interactions compete with ferromagnetic in-plane exchange, as usually observed in ferromagnetic perovskites [7–9].

On cooling (FC process), the magnetization follows a reversible path down to T_{rev} . At this temperature, the [Mn+Co] sublattice orders ferromagnetically ($T_c = T_{rev}$) and the magnetization increases abruptly, reaching higher values than those observed during the warming process. This process creates a local field (internal+applied) at the rare-earth site. The specific feature of both series presented in this work relates to the much higher magnetic moment of the rare-earth ion (Gd^{3+} or Er^{3+}) compared to the [Mn+Co] moment. Considering that the rare-earth ions behave as free spins, the thermal dependence of their magnetizations varies as $1/T$, that is, the magnetization increases and gradually overcomes the magnetization of the transition-metal sublattice, as the temperature decreases. By supposing a negative exchange interaction J between the [Mn+Co] and the RE moments, the rare-earth sublattice polarizes in the opposite direction to the local field, slowing down the magnetization increase of the ferromagnetic lattice. With further cooling, the overall magnetization reaches a maximum and starts to decrease, reaching the compensation temperature T_{comp} at $M = 0$, when the absolute values of both sublattices are fully equivalent. Upon further cooling, the magnetization becomes negative, in a so-called spin reversal phenomenon, when $M^{RE} > |M^{(Mn+Co)}|$.

We have developed a phenomenological model based on mean-field approximation to explain the spin reversal

in the lanthanide-substituted perovskites of the type $Gd_{1-x}Ca_xMnO_3$ [2]. Basically the same approach can apply to the present case, keeping in mind this time that the lanthanide network is 100% full and as such, its magnetization is higher than in the former case. In such an approximation, the local field at the RE site is imposed by the [Mn+Co] network and creates a magnetization $M^{RE} = \chi^{RE}(T) \cdot M^{Mn+Co}$. The total magnetization reads $M^{tot} = \{1 + |J| \chi^{RE}(T)\} M^{Mn+Co}$, where J is the negative exchange interaction between RE and [Mn+Co] spins. From this relation, it becomes immediately evident that, when $J < 0$ and at sufficiently low temperatures (that is, when the magnetic susceptibility of the lanthanide sublattice becomes very high), the total moment will reverse its sign.

At this point it is interesting to compare this behaviour with results obtained in the lanthanide-substituted manganites $Gd_{1-x}Ca_xMnO_3$ and $Er_{1-x}Ca_xMnO_3$ (Fig. 2, lower panels, [2]). In the gadolinium-based sample, similar mechanisms of magnetic exchange interaction as those exposed above may apply. However, in the case of $Er_{0.7}Ca_{0.3}MnO_3$, the magnetic moment of erbium clearly orients parallel and in the same direction as the moment due to the manganese sublattice. We are presently working on phenomenological models which could explain the particular behaviour of erbium, since it may present additive or opposite contributions, depending on the nature of the cationic substitution.

3.3. Magnetization loops

Fig. 3 shows the magnetization cycles performed on the same samples as described in Fig. 2. The upper and middle panels report data on $GdCo_xMn_{1-x}O_3$ and $ErCo_xMn_{1-x}O_3$, for $x = 0.3$ and 0.5 , while the lower panels show data for $Gd_{0.7}Ca_{0.3}MnO_3$, and $Er_{0.7}Ca_{0.3}MnO_3$. Some general features can be pointed out, in particular the superposition of two behaviours: one due to a ferromagnetic component, characterized by rather low coercive fields, and an antiferromagnetic component, characterized by a linear variation of M -versus- H at high fields. However, samples having an unchanged network at the B site ($RE_{1-x}Ca_xMnO_3$) present a much better-defined ferromagnetic cycle, extending up to 5–10 kOe. The partial substitution of manganese by cobalt, in a disordered fashion, obviously has an incidence on the ferromagnetic component, lowering the coercive field. At first sight, the cobalt spins seem to be oriented antiparallel to the manganese moments, enhancing the antiferromagnetic component and explaining the spin reversal observed for the erbium system when the substitution operates at the B-site.

By far, the most striking feature observed in the magnetization loops concerns the case of the $ErCo_xMn_{1-x}O_3$ solid solution. Two main phenomena can be described. Firstly, the magnetization branches intersect at about 7 kOe, for $T = 2$ K (upper left insert, Fig. 4);

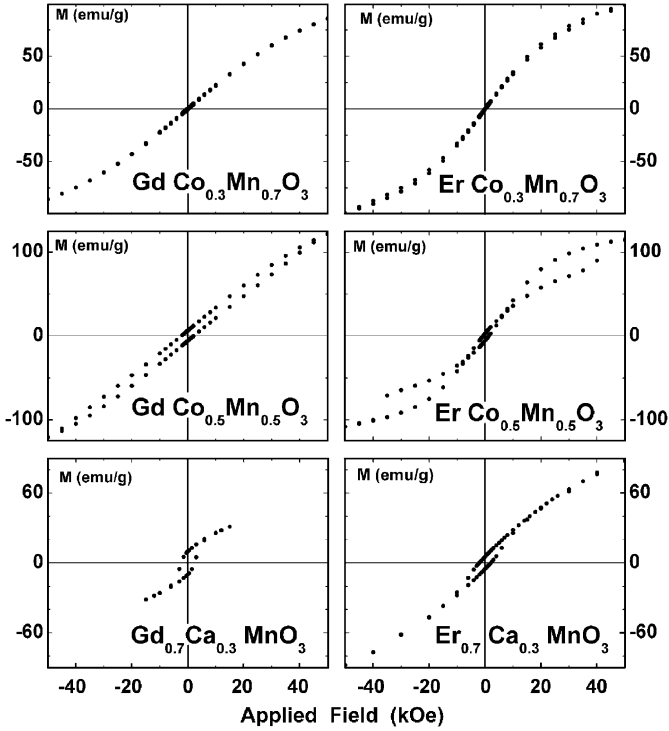


Fig. 3. Magnetization loops performed at 2 K ($\text{ErCo}_x\text{Mn}_{1-x}\text{O}_3$), 3.2 K ($\text{GdCo}_x\text{Mn}_{1-x}\text{O}_3$) and 5 K ($\text{RE}_{1-x}\text{Ca}_x\text{MnO}_3$).

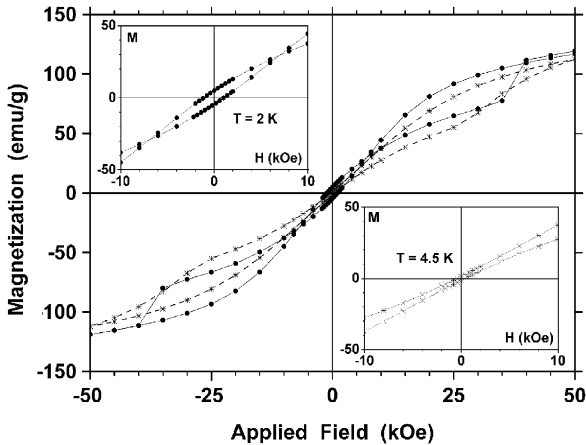


Fig. 4. Magnetization loops for $\text{ErCo}_{0.50}\text{Mn}_{0.50}\text{O}_3$ measured at 2 K (circles) and 4.5 K (crosses). Inserts show a zoom for $H \leq \pm 10$ kOe.

secondly, a sudden increase of the magnetization is observed at about ± 40 kOe, when the magnetic field increases (Fig. 4). The first phenomenon is clearly related to the spin reversal, since it disappears when the FC branch goes positive (lower right insert, Fig. 4). It is observed for compositions close to the 50/50 = Mn/Co ratio ($0.4 \leq x(\text{Co}) \leq 0.6$), although it is much more pronounced when the substitution is in a 1:1 ratio. Concerning the sudden increase of the magnetization at high fields, it is more likely to be related to a metamagnetic or spin-flop mechanism, that is, to a sudden re-orientation of the overall moments with respect to the applied field. Although this phenomenon is less pronounced for other compositions, it is still

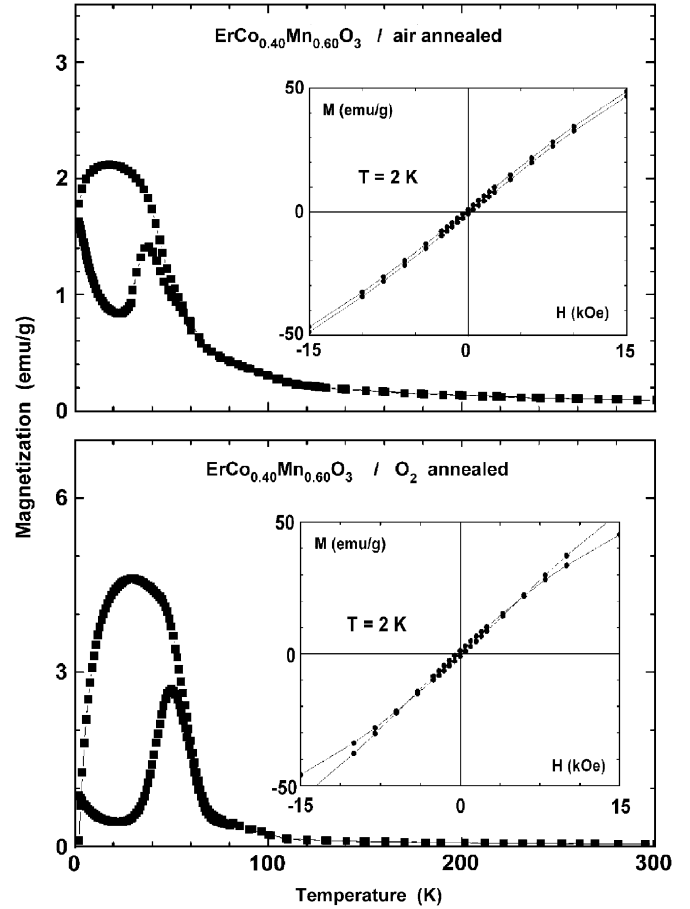


Fig. 5. Effect of annealing on the magnetization of $\text{ErCo}_{0.40}\text{Mn}_{0.60}\text{O}_3$. Insert shows low-field data of the magnetization loops performed at 2 K.

present for all samples of the $\text{ErCo}_x\text{Mn}_{1-x}\text{O}_3$ series studied in this work ($0.3 \leq x(\text{Co}) \leq 0.7$).

Annealing conditions may influence the ordered state, as noticed for the $\text{ErCo}_{0.40}\text{Mn}_{0.60}\text{O}_3$ composition (Fig. 5). The sample treated under oxygen (lower panel) clearly shows the intersection of the increasing and decreasing branches during the magnetization loop performed at 2 K, while the other one, treated under air (upper panel) does not show any crossing at low fields. Assuming that the annealing conditions favours the existence of Co^{3+} ions with respect to Co^{2+} [4], we may conclude that the anomalies observed in the magnetization cycles result in a subtle equilibrium between the magnetic moments of all ions (Er^{3+} , Mn^{3+} , Mn^{4+} , Co^{2+} and Co^{3+}) present in the sample.

We are presently working on this phenomenon, which needs to be studied on single crystals and at high magnetic fields. A thorough theoretical explanation is also under way, which takes into account the presence of all magnetic entities with the respective exchange interactions between species.

Acknowledgments

Authors acknowledge the France–Brazil program CAPES-COFECUB, project no. 416/03, the France–Spain

CNRS-CSIC program, project no. 18873, and the Région Bretagne for financial support. PB is greatly indebted to the French Ministry of Education and the UMR 6226 laboratory during her post-doctoral stay.

References

- [1] G.J. Snyder, C.H. Booth, F. Bridges, R. Hiskes, S. DiCarolis, M.R. Beasley, T.H. Geballe, *Phys. Rev. B* 55 (1997) 6453.
- [2] O. Peña, M. Bahout, K. Ghanimi, P. Duran, D. Gutierrez, C. Moure, *J. Mater. Chem.* 12 (2002) 2480.
- [3] O. Peña, M. Bahout, D. Gutierrez, P. Duran, C. Moure, *Solid State Sci.* 5 (2003) 1217.
- [4] C. Moure, D. Gutierrez, O. Peña, P. Duran, *J. Am. Ceram. Soc.* 86 (2003) 54.
- [5] O. Peña, K. Ghanimi, C. Moure, D. Gutierrez, P. Duran, *Bol. Soc. Esp. Ceram. V.* 43 (2004) 706.
- [6] M. Mouallem-Bahout, T. Roisnel, G. André, D. Gutierrez, C. Moure, O. Peña, *Solid State Commun* 129 (2004) 255 and references therein.
- [7] M. Hennion, F. Moussa, J. Rodriguez-Carvajal, L. Pinsard, A. Revcolevschi, *Phys. Rev. B* 56 (1997) R497.
- [8] B. Dabrowski, X. Xiong, Z. Bukowski, R. Dybzinski, P.W. Klamut, J.E. Siewenie, O. Chmaissem, J. Shaffer, C.W. Kimball, J.D. Jorgensen, S. Short, *Phys. Rev. B* 60 (1999) 7006.
- [9] J.M. De Teresa, C. Ritter, M.R. Ibarra, P.A. Algarabel, J.L. Garcia-Muñoz, J. Blasco, J. Garcia, C. Marquina, *Phys. Rev. B* 56 (1997) 3317.